OPTICAL CHARACTERIZATION OF NATIVE DEFECTS IN 4H-SiC IRRADIATED BY 10 MeV ELECTRONS WITH SUBSEQUENT ANNEALING

Y. Zhang [1], K. Wang [1*], H. Wang [1], Y. Tian [1,2], Y. Wang [3], J. Li [1*], Y. Chai [1]

[1] School of Materials Science and Engineering at Taiyuan University of Science and Technology, Taiyuan, Shanxi 030024, China; e-mail: wangkaiyue8@163.com, lijunlin9726@163.com
[2] Shanxi Engineering Vocational College, Taiyuan, Shanxi 030024, China
[3] The Second Research Institute of China Electronic Technology Group, Taiyuan, Shanxi 030024, China

Low-temperature photoluminescence was employed to investigate the defects of 4H-SiC crystals after high-energy electron irradiation, and the annealing characteristics and dependence of the detecting temperature and irradiation doses were investigated. Results showed that the emission, associated with carbon antisite–vacancy $(V_CC_{Si})^+$ defects was dominant in the electron-irradiated 4H-SiC crystal. With increase in detecting temperature, the emission decreased demonstrating red-shifted, and the full width at half-maximum broadened, which was attributed to the increase in the concentration of carriers arising from thermal activation at high temperature. The emission intensity was the highest value at an irradiation dose of 7.9×10^{18} e/cm^2, and then began to decrease. This revealed the lattice damage caused by long-term high-energy irradiation, which reduced the intensity of the defect radiation in the spectrum.

Keywords: *silicon carbide, photoluminescence, defect radiation, electron irradiation.*

ОПТИЧЕСКИЕ ХАРАКТЕРИСТИКИ СОБСТВЕННЫХ ДЕФЕКТОВ 4H-SiC, ОБЛУЧЕННОГО 10-МэВ ЭЛЕКТРОНАМИ С ПОСЛЕДУЮЩИМ ОТЖИГОМ

Y. Zhang [1], K. Wang [1*], H. Wang [1], Y. Tian [1,2], Y. Wang [3], J. Li [1*], Y. Chai [1]

УДК 535.37

[1] Школа материаловедения и инженерии Тайюаньского университета науки и технологий, Тайюань, Шаньси 030024, Китай; e-mail: wangkaiyue8@163.com, lijunlin9726@163.com
[2] Инженерный профессиональный колледж Шаньси, Тайюань, Шаньси 030024, Китай
[3] Второй научно-исследовательский институт Китайской группы электронных технологий, Тайюань, Шаньси 030024, Китай

(Поступила 23 июля 2019)

Для исследования дефектов кристаллов 4H-SiC использована низкотемпературная фотолюминесценция после облучения высокоэнергетическими электронами. Изучены характеристики отжига и зависимость температуры детектирования от доз облучения. Результаты показывают, что в облученном электронами кристалле 4H-SiC доминирует эмиссия, связанная с дефектами углеродная антиструктура—вакансия $(V_CC_{Si})^+$. С повышением температуры детектирования излучение уменьшается и сдвигается в красную область, а полная ширина на полувысоте увеличивается, что связано с повышением концентрации носителей в результате термической активации при высокой температуре. Интенсивность излучения максимальна при дозе облучения $7.9\cdot10^{18}$ эл/см^2, затем она уменьшается. Это свидетельствует о повреждении решетки, вызванном длительным высокоэнергетическим облучением, что уменьшает интенсивность радиационного дефекта в спектре.

Ключевые слова: *карбид кремния, фотолюминесценция, радиационный дефект, электронное облучение.*

Introduction. As an important wide-bandgap semiconductor, silicon carbide (SiC) has been applied in many areas, such as high-frequency and high-power microelectronic devices and optoelectronic devices [1–4]. The properties of the intrinsic defects in a SiC crystal play an important role in these applications; for instance, carrier traps and recombination centers of intrinsic defects in high-quality 4H-SiC can shorten the lifetime of minority carriers and make the open-state voltage drop of high voltage bipolar transistors very small [5, 6]. Therefore, it is important to study the intrinsic defects of SiC. Photoluminescence (PL) technology is sensitive to crystal defects and does not destroy the crystal structure; thus, it is suitable for the characterization of crystal defects.

To explore the properties of defects, intrinsic defects are usually introduced into crystals artificially. In previous studies, the most commonly used method is near displacement threshold electron irradiation using a transmission electron microscope. This method can introduce some simple intrinsic defects successfully into a crystal, such as carbon vacancies, silicon vacancies, and interstitial defects [7–9].

Semiconductor devices are usually irradiated by MeV order of magnitude ultra-high electron energy; however, there are few studies concerning the defects created with high-energy irradiation on SiC. In this paper, intrinsic defects are created by 10 MeV high-energy electron irradiation on a 4H-SiC crystal, which are then characterized by low-temperature photoluminescence spectroscopy. The results are analyzed and discussed.

Experimental methods. This work focused on the 3-inch high-purity 4H-SiC substrates, which were grown through (0001) plane epitaxy using the physical vapor transport method by the Second Research Institute of China Electronics Technology Group Corporation. The substrates were divided into six groups for 10-MeV high-energy electron irradiation. The irradiation was performed with a power of 80 kW at room temperature, and the irradiation times were set as 1, 2, 3, 4, 5, and 6 h. The whole surface of 4H-SiC films was irradiated by the electron beam. The irradiation doses for the six specimens were as follows: 2.6×10^{18}, 5.3×10^{18}, 7.9×10^{18}, 1×10^{19}, 1.3×10^{19}, and 1.6×10^{19} e/cm^2.

The samples were annealed after electron irradiation by an RT-1200 rapid annealing furnace in an argon gas flow for 30 min. The temperatures ranged from 400 to 900°C, in steps of 100°C. After the irradiation, these samples were cut into several slices of size 5×5×0.2 mm and transferred to micro-Raman spectrometers (Renishaw) fitted with cryogenic stages (Linkam Instruments), which could be cooled to about approximately 77 K with liquid nitrogen cooling. The samples were irradiated with a Nd semiconductor laser at 532 nm. The procedure of PL operation analysis involves the cooling down of samples to 110 K. The resolution of the optical system was degraded by the cryostats to an approximately 1 μm lateral resolution of approximately 1 μm. The samples were studied in back reflection mode with the irradiated face, mostly (0001), perpendicular to the incident laser beam or with the sample mounted so that the laser beam was incident perpendicular to the usual direction of electron irradiation. The laser polarization was either perpendicular or parallel to [0001].

Results and discussions. Figure 1 presents the typical PL spectra of 4H-SiC without irradiation and with 3 h irradiation (dose 7.9×10^{18} e/cm^2). In addition to the original TO and LO Raman modes of 4H-SiC at 555.1 and 560.9 nm with two second-order structured bands situated at 578.9 and 584.7 nm (inset in Fig. 1a), seven new zero phonon lines appeared in the range of 645–690 nm after irradiation, which were located at 649, 652.2, 665.2, 672, 673.2, 675.5, and 676.8 nm. The inset in Fig. 1b shows that the profile of the first three lines were similar, and the last four lines had similar asymmetric profiles. Thus, the lines were labeled as $A1$ = 649 nm, $A2$ = 652.2 nm, $A3$ = 665.2 nm and $B1$ = 672 nm, $B2$ = 673.2 nm, $B3$ = 675.5 nm, and $B4$ = 676.8 nm, which were referred to as A and B emissions. There were complex vibrational structures behind the seven peaks (from 680 to 725 nm).

Moreover, the effect of the irradiation dose on the crystal defects was studied, as shown in Fig. 2. When the irradiation time was 3 h, the intensity of the A and B peaks was the strongest, but the spectrum was considerably quenched with an increased irradiation time. For instance, the intensity of the $B3$ peak was enhanced up to 28838 a. u. at 3-h irradiation, but the intensities weakened to 11153, 8153, and 5762 a. u. at 4, 5, and 6 h, respectively. Consequently, when the irradiation dose was 7.9×10^{18} e/cm^2, the best luminescent efficiency for A and B emissions was achieved.

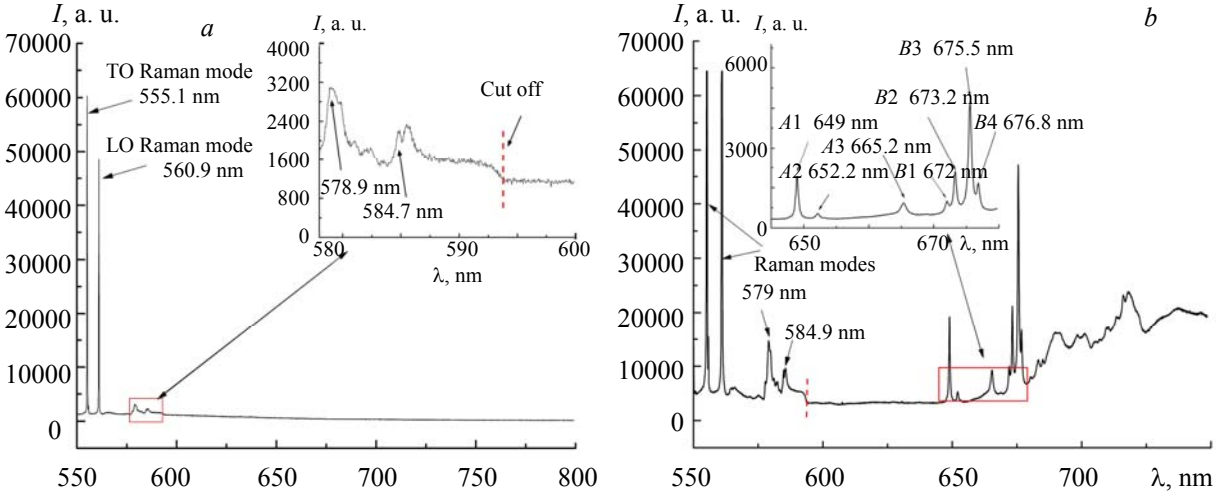

Fig. 1. Typical spectra of the 4H-SiC without (a) and with (b) irradiation obtained with excitation at 532 nm and temperature of ~110 K.

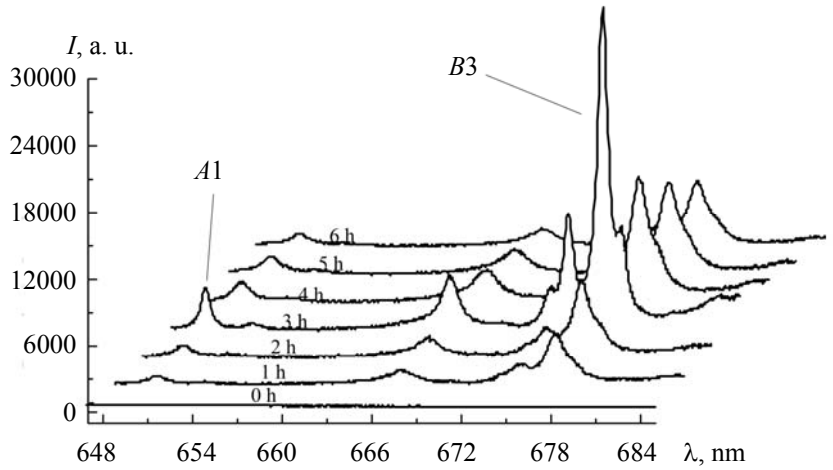

Fig. 2. Spectra of *AB* emissions at different irradiation times obtained with excitation at 532 nm and temperature of ~110 K.

To further explore the characteristics of the *A* and *B* emissions, the sample with the best luminescence efficiency was selected to investigate the detecting temperature dependence. Figure 3a presents the PL spectra of the sample irradiated for 3 h obtained with excitation at 532 nm and a temperature of 110–250 K. With increase in temperature, the *A* and *B* peaks exhibited a red shift, together with intensity quenching and an increase in the full width at half-maximum (FWHM). With regard to the increase in the FWHMs, Lorentzian fit was employed to fit the FWHMs of the *A* and *B* peaks. Figure 3b shows the Lorentzian analysis performed on the *A*1 lines at 110–250 K, and the precision was over 95%. The Lorentzian function is defined as

$$y = y_0 + \frac{2A}{\pi}\frac{w}{4(x - x_c)^2 + w^2},$$

where y_0 and x_c are the offset and center of the Lorentzian curve, respectively, while w and A are the width and area of the Lorentzian curve, respectively.

The fitted values of the FWHMs were further processed, as shown in Fig. 3c. The *y*-axis was calibrated to all FWHM values by subtracting the value at 110 K. A third-order nonlinear fitting of the scatter points was also carried out, and a fitting accuracy of 98% was achieved. It was observed that as the characterization temperature increased, the broadening of FWHMs showed a nonlinear growth.

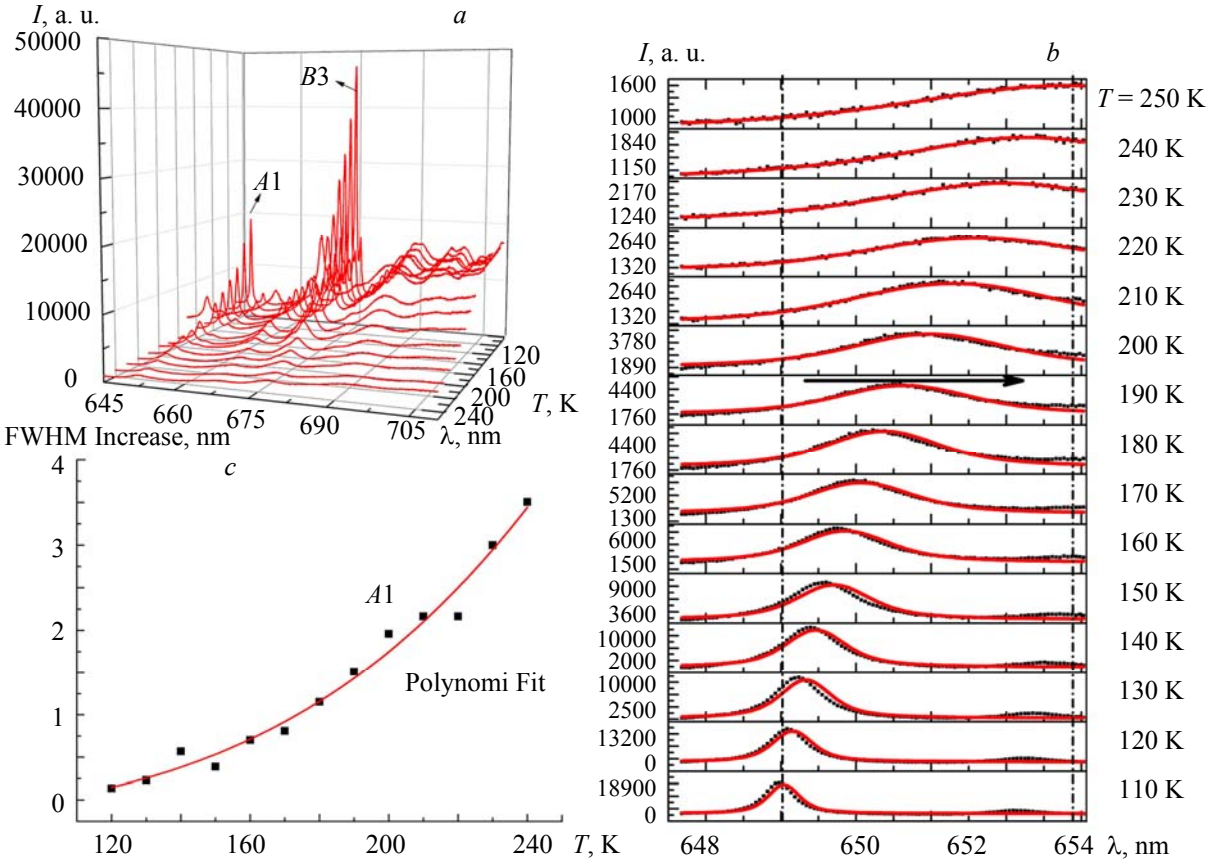

Fig. 3. a) Full PL spectra of the *A* and *B* emissions recorded at 110–250 K; b) Lorentzian curve fitting for the *A*1 peak; c) temperature dependence of Lorentzian FWHMs of the *A*1 peak.

Furthermore, annealing was carried out on the crystals irradiated for 3 h. At a suitable annealing temperature, interstitial atoms and vacancies are activated to diffuse, which resulted in a variation of the luminescence defects. The typical PL spectra of the sample after annealing at 400–900 °C are displayed in Fig. 4. The *A* and *B* lines exhibited a consistent annealing behavior, and the intensities reached a maximum at 700°C. However, the *AB* lines revealed the onset of thermal quenching on annealing up to 800°C.

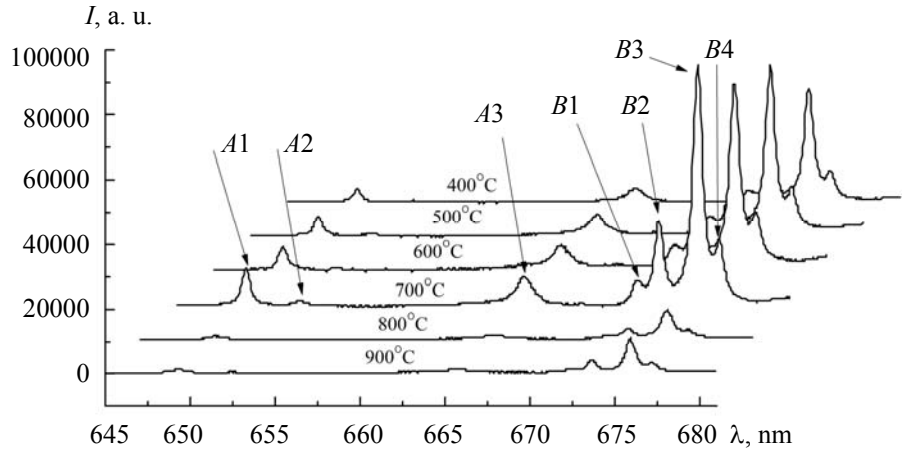

Fig. 4. Full spectra of *AB* emissions at different annealing temperatures obtained with excitation at 532 nm and temperature of ~110 K.

The PL spectrum of pure 4H-SiC should only consist of TO and LO Raman modes [10], which appear at 555.1 and 560.9 nm upon excitation by a 532-nm laser. After irradiation, the FWHMs of the Raman modes were broadened from 0.26 and 0.25 to 0.47 and 0.66 nm, and the intensities of the second-order structured bands were increased from 3098.1 and 2292 to 14760.3 and 9613.7 a. u., respectively (Fig. 1).

The carbon or silicon atoms at the 4H-SiC crystal lattice points broke away from the lattice with sufficient doses of energetic electron bombardment and became interstitial atoms with a vacancy formed at the lattice point. After irradiation, the *A* and *B* emissions centers were exhibited by the crystal, so the defect was related to self-interstitials or vacancies. When the sample was irradiated for 3 h, the best radiation effect of introducing the *A* and *B* defects into the crystal was achieved (Fig. 2). In addition, irradiation for a long period caused lattice damage, which resulted not only in the introduction of point defects into the crystal but also the formation of dislocations that destroyed the crystal structure.

At a sufficiently low temperature, the photoluminescence of the defects is only a zero-phonon transition, and the multi-phonon transition requires a higher activation energy [11]. Therefore, the emissions observed at cryogenic temperature were strong and sharp, but with increase in temperature, the multi-phonon transitions began to dominate, which resulted in the decrease in the vibration energy of the *A* and *B* emissions [12]. Additionally, all peaks were red-shifted by approximately 3.8 nm (Fig. 3a). The coincident temperature dependence of the *A* and *B* emissions indicated that they originated from a crystal defect.

In addition, a distinction between the inhomogeneous and homogeneous broadening mechanisms for the FWHMs broadening should be made [13]. Homogeneous broadening is one of the ultimate consequences of the electron-phonon coupling, and inhomogeneous broadening is the result of strains and defects randomly distributed in crystal hosts [14]. The interaction of the active ions with phonons in equivalent sites, and thus with the same probability, results in a temperature-dependent Lorentzian shape of the emission. Therefore, this type of line broadening is regarded as homogeneous broadening [15].

According to the fitting results, the FWHM was only 0.23 nm at 110 K, but the FWHM was broadened to 3.64 nm when the temperature was increased to 250 K (Fig. 3b). With increase in temperature, the intrinsic carrier concentration in the crystal increased, and the electron-phonon coupling became stronger, which showed a homogeneous broadening mechanism. This also illustrates that the *AB* emission was an intrinsic defect in the SiC crystal. There was an obvious wide sideband behind the *AB* emission, which indicated the emission peaks were caused by vacancy-related defects [16].

Furthermore, the identical annealing properties of the *A* and *B* emissions certified that all peaks originated from the same defect (Fig. 4). Thus, the *A* and *B* lines were collectively referred to as *AB* emissions. During the annealing from 400 to 700 °C, the movement of interstitial atoms promoted the formation of *AB* defects and enhanced the luminescence efficiency. However, when the annealing was up to 800°C, the intensities of the peaks decreased. It has been established that *AB* emission is created by the on-axis and off-axis carbon antisite–vacancy (CAV) pairs, $V_C C_{Si}$ [17]. Castelletto et al. revealed the four possible atomistic models and the electronic structure for configurations (both axial and basal plane) of the $V_C C_{Si}$, and the CAV defect was positively charged [18].

The displacement thresholds of Si and C in SiC crystals were 250 and 100 keV, respectively. Therefore, carbon vacancies (V_C) and silicon vacancies (V_{Si}) were produced during electron irradiation. The minimum irradiation energy of V_C formation was 0.3 MeV, which was lower than that of the V_{Si} formation energy (0.5 MeV) [19]. It was found that the instability of V_{Si} caused the adjacent carbon atoms to leave their lattice positions, occupy V_{Si} to form C_{Si}, and left a vacancy (V_C), which resulted in the $V_C C_{Si}$ defect [20].

Conclusions. The crystal defects of 4H-SiC were characterized by Raman spectroscopy. The effects of irradiation dose and annealing characteristics and the temperature dependence of defects were studied by low-temperature photoluminescence. The results showed that after electron irradiation, obvious *AB* emissions appeared in the spectra, which were caused by the intrinsic defect of $(V_C C_{Si})^+$. The temperature dependence of *AB* emissions showed the decrease in intensity, red shift, and FWHMs broadening with increasing temperature. This was caused by the increase in carrier concentration arising from thermal activation at high temperature. In addition, the effect of irradiation dose showed that the intensity of *AB* emissions reached a maximum at a dose of 7.9×10^{18} e/cm^2. This revealed lattice damage was caused by high-energy irradiation for too long a duration and reduced the intensity of the defect radiation in the spectrum.

Acknowledgments. This study was funded by Fund Program for the Scientific Activities of Selected Returned Overseas Professionals in Shanxi Province (No. 20200024), Research Project Supported by Shanxi Scholarship Council of China (No. 2020-129), Shanxi Postgraduate Innovation Project (No. 2020SY413, 2020BY107), and the Key Research and Development Projects of Shanxi Province (No. 201803D121027).

REFERENCES

1. Y. Zhou, H. Hyuga, D. Kusano, Y. Yoshizawa, T. Ohji, K. Hirao, *J. Asian Ceram. Soc.*, **3**, 221–229 (2015).
2. Z. Huang, X. Zhang, T. Wang, G. Liu, H. Shao, Y. Wan, G. Qiao, *Surf. Coat. Technol.*, **335**, 198–204 (2018).
3. A. Gali, *J. Mater. Res.*, **27**, 897–909 (2012).
4. W. F. Koehl, B. B. Buckley, F. J. Heremans, G. Calusine, D. D. Awschalow, *Nature*, **479**, 84–87 (2011).
5. A. Ellison, B. Magnusson, N. T. Son, L. Storasta, E. Janzén, *Mater. Sci. Forum*, **433-436**, 33–38 (2003).
6. St. G. Müller, M. F. Brady, W. H. Brixius, R. C. Glass, H. Mc D. Hobgood, J. R. Jenny, R. T. Leonard, D. P. Malta, A. R. Powell, V. F. Tsvetkov, S. T. Allen, J. W. Palmour, C. H. Carter, Jr., *Mater. Sci. Forum*, **433-436**, 39–44 (2003).
7. J. W. Steeds, F. Carosella, A. G. Evans, M. M. Ismail, L. R. Danks, W. Voegeli, *Mater. Sci. Forum*, **353-356**, 381–384 (2001).
8. N. T. Son, P. N. Hai, E. Janzén, *Phys. Rev. B*, **63**, 201201(R) (2011).
9. A. Mattausch, M. Bockstedte, O. Pankratov, J. W. Steeds, S. Furkert, J. M. Hayes, W. Sullivan, N. G. Wright, *Phys. Rev. B*, **73**, 161201(R) (2006).
10. S. Nakashima, H. Harima, *Phys. Status Solidi (a)*, **162**, 39–64 (1997).
11. J. Steeds, K. Wang, Z. Li, *Diamond Relat. Mater.*, **23**, 154–156 (2012).
12. H. Wang, F. D. Medina, D. D. Liu, Y. Zhous, *J. Phys.: Condens. Matter*, **6**, 5373–5386 (1994).
13. J. Garcia Solè, L. E. Bausà, D. Jaque, *An Introduction to the Optical Spectroscopy of Inorganic Solids*, Wiley, New York (2005).
14. M. Marco, M. Marianna, C. R. Pier, A. Alberto, *J. Phys.: Condens. Matter*, **24** 135401 (2012).
15. R. C. Powell, *Physics of Solid State Laser Materials*, Springer Verlag, New York (1998).
16. J. W. Steeds, W. Sullivan, S. A. Furkert, G. A. Evans, *Phys. Rev. B*, **77**, 195203 (2008).
17. J. W. Steeds, *Phys. Rev. B*, **80**, 245202 (2009).
18. S. Castelletto, B. C. Johnson, V. Ivády, N. Stavrias, T. Umeda, A. Gali, T. Ohshima, *Nature Mater.*, **13**, 151–156 (2014).
19. H. Iuni, H. Mori, H. Fujita, *Philos. Mag. B*, **61**, 107–124 (1990).
20. M. V. B. Pinheiro, E. Rauls, U. Gerstman, S. Greulich-Weber, H. Overhof, J.-M. Spacth, *Phys. Rev. B*, **70**, 245204 (2004).